# Quantum Spin Liquid Intertwining Nematic and Superconducting Order in Fese

Jian-Huang She, Michael J. Lawler, and Eun-Ah Kim

Phys. Rev. Lett. **121**, 237002 — Published 7 December 2018

DOI: 10.1103/PhysRevLett.121.237002

# Quantum spin liquid intertwining nematic and superconducting order in FeSe

Jian-Huang She[1], Michael J. Lawler[2,1,3], and Eun-Ah Kim[1,3]
[1] *Department of Physics, Cornell University, Ithaca, NY 14853, USA*
[2] *Department of physics, Binghamton University, Vestal, NY 13850, USA*
[3] *Kavli Institute for Theoretical Physics, Kohn Hall University Of California Santa Barbara CA 93106-4030, USA*
(Dated: October 26, 2018 [file: FeSe-main])

Despite its seemingly simple composition and structure, the pairing mechanism of FeSe remains an open problem due to several striking phenomena. Among them are nematic order without magnetic order, nodeless gap and unusual inelastic neutron spectra with a broad continuum, and gap anisotropy consistent with orbital selection of unknown origin. Here we propose a microscopic description of a nematic quantum spin liquid that reproduces key features of neutron spectra. We then study how the spin fluctuations of the local moments lead to pairing within a spin-fermion model. We find the resulting superconducting order parameter to be nodeless $s \pm d$-wave within each domain. Further we show that orbital dependent Kondo-like coupling can readily capture observed gap anisotropy. Our prediction calls for inelastic neutron scattering in a detwinned sample.

The pairing mechanism and gap symmetry of bulk[1–3] and single layer[4] FeSe is an open issue that inhibits an overarching understanding of iron-based superconductors. Although a spin-fluctuation mediated pairing scenario is a broadly accepted mechanism in iron-based superconductors,[5,6] much debate continues to focus around two distinct perspectives: weak coupling and strong coupling. Weak coupling approaches are sensitive to the band structure and generally predict dominantly $(\pi, 0)$, $(0, \pi)$ spin density wave fluctuations that couple hole pockets to electron pockets in all Fe-pnictides as well as in bulk FeSe.[7] Strong coupling approaches take strong electron-electron correlations to generate quasi-localized moments that would interact with itinerant carriers.

FeSe presents new challenges to both perspectives, including explaining its nematic order[8](see Fig. 1(a)), its absence of magnetism, its gapped but active spin fluctuations at $(\pi, \pi)$ in addition to $(\pi, 0)$[9] and its nodeless superconducting gap. There have been much efforts to address these issues. RPA based weak-coupling approaches focused on implications of assumed nematic order.[10,11] Renormalization group approaches found the effective interactions promoting spin density wave to be also promoting orbital order.[7,12,13] Approaches focusing on sizable local moments[14] led to proposals of quadrupolar order accompanying nematic order[15,16] and the proposal of a quasi-one dimensional quantum paramagnet state[17] of AKLT (Affleck-Kennedy-Lieb-Tasaki)[18] type. Nevertheless, strikingly unique inelastic neutron spectra (INS) of FeSe evade the approaches so far one way or another.

The absence of the stripe order in FeSe has been attributed to the notion of frustration.[17,19] Indeed FeSe is close to a classic situation for frustrated magnets in the much studied $J_1$-$J_2$ model[20,21](see Fig. 1(b)). Interestingly, in systems that form stripe upon cooling, viewing the nematic state as thermally melted version of stripe was a very productive point of view.[22] Here we note that frustration from the competition between $J_1$ and $J_2$ has been long known to drive quantum melted versions of Neel and stripe orders giving rise to $C_4$ symmetric and $C_2$ symmetric (nematic) quantum spin liquids (QSL) respectively.[23,24] Moreover DMRG studies on $J_1$-$J_2$ model noted an intermediate paramagnetic phase between stripe order and Neel order state.[25,26] A recent DMRG study of $J_1$-$J_2$-$K_1$-$K_2$ spin model found a nematic quantum paramagnetic state between the Neel and stripe ordered states.[27] However, no link between the notion of frustration and the intriguing INS or superconductivity has been established theoretically. In this letter we propose a microscopic (lattice model) description of the frustration driven nematic quantum spin liquid (QSL) state that amounts to quantum melted stripe and captures the observed INS. We then show that this nematic quantum liquid state intertwines nematic order and superconductivity in the charge sector, as the anisotropic spin fluctuation breaks the point group symmetry and mediate superconductivity at once.

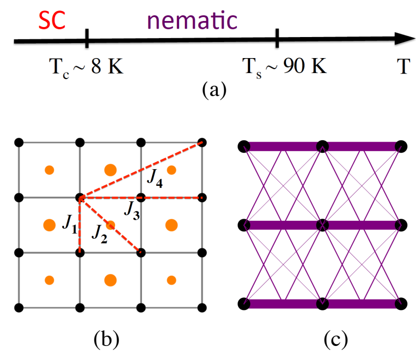


FIG. 1. (Color online) (a) Phase diagram of FeSe. (b) Lattice structure of FeSe. The black dots represent Fe atoms, and the orange dots represent Se atoms above and below the Fe plane. $J_{1-4}$ denote the exchange couplings. (c) The nematic quantum spin liquid state of FeSe. The purple solid lines represent antiferromagnetic bonds, with their thickness proportional to bond strength.

In FeSe, there is evidence that local moments[14] coexist with itinerant carriers of all three $t_{2g}$ orbitals.[28–30] In order to capture the dual character[31] we turn to a spin-

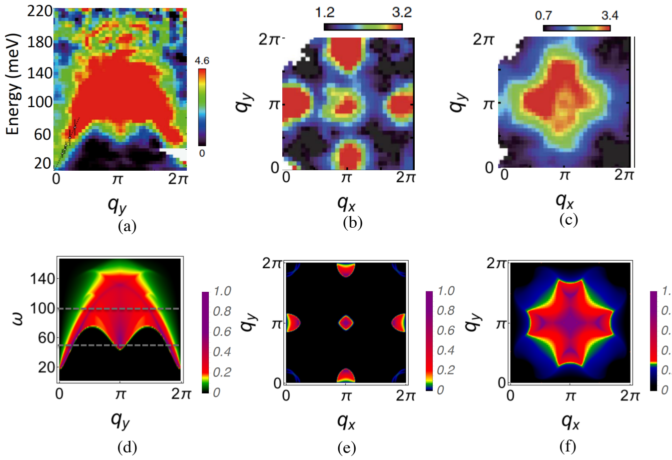


FIG. 2. (Color online) (a, b, c): Neutron scattering results for the dynamic spin structure factor $\mathcal{S}(q_x, q_y, \omega)$ at $q_x = \pi$ (a), $\omega = 50, 100$ meV (b, c).[9] (d, e, f): SBMFT structure factor for the $J_1$-$J_2$-$J_3$-$J_4$ model at $J_2/J_1 = 0.904$, $J_4/J_1 = 0.975$ (the $J_3$ term drops out of the mean field level) and "spin" $S = 0.153$. These results are summed over two nematic domains.

fermion model:[32–37] $\mathcal{H} = \mathcal{H}_c + \mathcal{H}_S + \mathcal{H}_{\rm int}$, where $\mathcal{H}_c$ and $\mathcal{H}_S$ describe the itinerant carriers and local moments respectively that are coupled through $\mathcal{H}_{\rm int}$. For the spin model

$$\mathcal{H}_S = \sum_{ij} J_{ij} \boldsymbol{S}_i \cdot \boldsymbol{S}_j, \tag{1}$$

with exchange interactions $J_{ij}$ on a square lattice (Fig.1(b)), the two dominant interactions are the nearest-neighbor $J_1$ and the next-nearest-neighbor $J_2$ exchange interactions as in other Fe-based superconductors.[38,39] But due to the near itinerancy of the core electrons, longer range terms are also expected.[19] Here we keep $J_1, J_2, J_3, J_4$ terms (Fig.1(b)).

The $J_1$-$J_2$ model has been extensively studied both classically and quantum mechanically (see Refs.[20, 21, 25, and 26]). Within classical models the role of frustration is clear from the fact that the model can be recast as $\mathcal{H}_S = J_2 \sum (\boldsymbol{S}_1 + \boldsymbol{S}_2 + \boldsymbol{S}_3 + \boldsymbol{S}_4)^2$ up to a constant at $J_2 = J_1/2$ point, where $\boldsymbol{S}_{1-4}$ are the four spins on each plaquette $\langle 1234 \rangle$ and the summation is over all plaquettes. Classical ground state with vanishing total spin on each plaquette property leads to a zero mode at each wave vector on the Brillouin zone boundary[21] and so the model is highly frustrated. With quantum effects of small spin $S$ the frustration effects are not limited to the fine tuned point of $J_2 = J_1/2$. Unfortunately, a controlled theoretical study for quantum spins for such frustrated spin systems is challenging. Hence we will restrict ourselves to mean field theories and choose an ansatz that (1) agrees with the observed inelastic neutron spectrum,[9] and (2) the ordering tendencies obey the classical condition of $\boldsymbol{S}_1 + \boldsymbol{S}_2 + \boldsymbol{S}_3 + \boldsymbol{S}_4 = 0$ on a plaquette.

A prominent feature of the INS data[9] is its broad and gapped continuum of spectral weight (Fig.2a) without any one-magnon branch. Intriguingly such a continuum is expected in a QSL with deconfined spinons in two-dimension in an insulating magnetic system.[40] Indeed it is a common feature of slave-particle mean field theories. So we will choose Schwinger boson mean field theory (SBMFT)[41] as our mean field theory approach. Additional features of Fig. 2 (a-c) we aim to capture include: (1) The simultaneous presence of both $(\pi, \pi)$ spin fluctuations and $(\pi, 0)$, $(0, \pi)$ spin fluctuations. (2) The quasi-one-dimensional dispersion $\omega \sim \sin k_y$[42–44] found in the shape of the upper and lower bounds. (3) The observed cross-shaped spectrum around $(\pi, \pi)$.

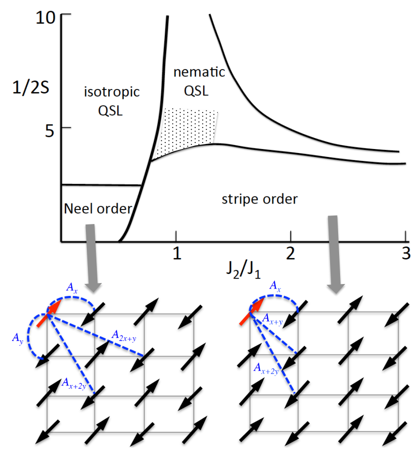


FIG. 3. (Color online) (top) The SBMFT phase diagram of the $J_1$-$J_2$ model.[45] Our mean field ansatz is the shaded region with added terms for the J3 and J4 exchange interactions. (bottom) The spin configurations in the two long-range ordered phases. The blue dashed lines represent the mean field bonds connecting a spin (red arrow) with its neighboring spins (black arrows). Here Neel order, stripe order, isotropic QSL, nematic QSL correspond respectively to $(\pi, \pi)_{\rm LRO}$, $(\pi, 0)_{\rm LRO}$, $(\pi, \pi)_{\rm SRO}$, $(\pi, 0)_{\rm SRO}$ in.[45]

To find these features in a SBMFT, we turn to the known[45] SBMFT phase diagram of the $J_1$-$J_2$ model (Fig. 3). Note that the Neel and stripe long range order for small $J_2/J_1$ and large $J_2/J_1$ are expected[24] to melt into $C_4$ symmetric and $C_2$ symmetric QSL's respectively (see Fig. 3). Hence the shaded region near the phase boundary between $C_4$ symmetric QSL, $C_2$ symmetric QSL and the stripe ordered phase will capture all of the above features. Specifically, states in this region will support a dynamic spin structure factor with 1d-like dispersion and cross-shaped spectrum *assuming twin domains of the stripe state are averaged over in the INS data.* To account for the itinerancy of the electrons, we extend an ansatz within the shaded region of Fig. 3 with the additional $J_3$ and $J_4$ neighbor couplings. We also note the small value of $2S$ in the phase diagram (i.e. $S \approx 0.15$) corresponds to mean field theory over emphasizing the stability of the ordered phase.

To construct the ansatz, we now turn briefly to the specifics of SBMFT. In Schwinger boson representation, each spin $\boldsymbol{S}_{\mathbf{r}}$ is represented by two bosonic operators $b_{\mathbf{r}\sigma}$, $\sigma =\uparrow,\downarrow$ with the constraint $\sum_\sigma b^\dagger_{\mathbf{r}\sigma} b_{\mathbf{r}\sigma} = 2S$. The spin operator is then $\boldsymbol{S}_{\mathbf{r}} = \frac{1}{2}\sum_{\sigma\sigma'} b^\dagger_{\mathbf{r}\sigma}\boldsymbol{\sigma}_{\sigma\sigma'} b_{\mathbf{r}\sigma'}$, with $\boldsymbol{\sigma}$ the Pauli matrices. We can then expand $H_{\mathbf{r},\mathbf{r}'} \equiv J_{\mathbf{r},\mathbf{r}'}\boldsymbol{S}_{\mathbf{r}}\cdot\boldsymbol{S}_{\mathbf{r}'}$ in terms of the spin singlet operator $A^\dagger_{\mathbf{r},\mathbf{r}'} = b^\dagger_{\mathbf{r}\uparrow}b^\dagger_{\mathbf{r}'\downarrow} - b^\dagger_{\mathbf{r}\downarrow}b^\dagger_{\mathbf{r}'\uparrow}$ to obtain $H_{\mathbf{r},\mathbf{r}'} = -J_{\mathbf{r},\mathbf{r}'}\frac{1}{2}A^\dagger_{\mathbf{r},\mathbf{r}'}A_{\mathbf{r},\mathbf{r}'} + S^2$. Finally, we mean-field decompose $H_{\mathbf{r},\mathbf{r}'}$ and introduce mean fields $\langle A_{\boldsymbol{r},\boldsymbol{r}'}\rangle$ using $A^\dagger_{\mathbf{r},\mathbf{r}'}A_{\mathbf{r},\mathbf{r}'} = \langle A^\dagger_{\mathbf{r},\mathbf{r}'}\rangle A_{\mathbf{r},\mathbf{r}'} + A^\dagger_{\mathbf{r},\mathbf{r}'}\langle A_{\mathbf{r},\mathbf{r}'}\rangle - \langle A^\dagger_{\mathbf{r},\mathbf{r}'}\rangle\langle A_{\mathbf{r},\mathbf{r}'}\rangle$. We assume the bosons do not condense.

Defining $A_{\hat\mu} \equiv \langle A_{\boldsymbol{r},\boldsymbol{r}+\hat\mu}\rangle$, we keep $A_{\hat x} \neq 0$ and the diagonals $A_{\hat x\pm\hat y} \neq 0$ and $A_{\hat x\pm 2\hat y} \neq 0$ for states in the shaded region of Fig. 3. The fourth neighbor term can be understood as a result of the competition between Neel and stripe states: it is a bond that is favored by both the $(\pi,\pi)$ Néel state and the $(\pi,0)/(0,\pi)$ stripe state. The result is a state with the same projective symmetry group as the Read and Sachdev state used in the phase diagram of Fig. 3. It is a "zero flux state"[46] and hence energetically competitive. However, a full assessment of which QSL state produces the best fit to the neutron scattering data in Fig. 2 is beyond our scope. Our aim is to show that a quantum spin liquid better fits the data than current proposals. Most importantly it is a state in which translational symmetry is restored by quantum melting stripe into $C_2$ symmetric nematic QSL state.

We can then calculate the dynamic spin structure factor $\mathcal{S}_{\boldsymbol{q}\omega} \equiv \mathrm{Im}\langle S^z(\boldsymbol{q},\omega)S^z(-\boldsymbol{q},\omega)\rangle$ associated with our ansatz. At $T=0$, it is of the form[47] $\mathcal{S}_{\boldsymbol{q}\omega} \sim$

$$\sum_{\boldsymbol{k}} \left\{\cosh\left[2\left(\theta_{\boldsymbol{k}} + \theta_{\boldsymbol{k}+\tilde{\boldsymbol{q}}}\right)\right] - 1\right\}\delta\left(\omega_{\boldsymbol{k}} + \omega_{\boldsymbol{k}+\tilde{\boldsymbol{q}}} - |\omega|\right), \quad (2)$$

where $\theta_{\boldsymbol{k}}$ is the angle in the Bogoliubov transformation of SBMFT (see SM1 for explicit expression), and $\tilde{\boldsymbol{q}} = \boldsymbol{q} - (\pi,0)$ arises because of a standard unitary transformation we carried out on the B sublattice for simplicity. The results summing over two domains are plotted in Fig. 2(d-f). They capture the basic features of the neutron spectra: (1) The spectrum is gapped (Fig. 2d), as a result of the absence of long range magnetic ordering. (2) Both $(\pi,\pi)$ and $(\pi,0)/(0,\pi)$ spin fluctuations are present (Fig. 2d, e). (3) The spectrum displays the novel feature of continuum with the bounds exhibiting quasi-one-dimensional dispersion (Fig. 2d).

A sharp prediction of our model is the dramatic suppression of spectral weight around $(0,q_y)$ in a detwinned sample ($(q_x,0)$ for the other domain). This means at low energies there are weights at say $(\pi,\pi)$ and $(\pi,0)$, but not at $(0,\pi)$. By contrast, in an orbital order driven picture for nematic ordering, there is only a weak anisotropy in the spin-structure factor with the spectral weight at $(\pi,\pi)$, $(0,\pi)$ and $(\pi,0)$ of roughly the same magnitude even in a single nematic domain.[10,11] Such a distinction has profound implications for pairing. When the degree of anisotropy in the momentum distribution of the spin spectra is mild, pairing interactions with different $\boldsymbol{q}$-wavevectors compete, leading to nodes.[10,11] On the other hand, the strong anisotropy in the spectral weight distribution in our SBMFT ansatz removes a need for a superconducting gap node. (See SM3.)

We now turn to the itinerant degrees of freedom to study nematicity and superconductivity. Their kinetic energy is given by a tight-binding model:

$$\mathcal{H}_c = \sum_{\boldsymbol{k},\alpha\beta,\nu} \epsilon^{\mu\nu}_{\alpha\beta}(\boldsymbol{k})c^\dagger_{\alpha\mu}(\boldsymbol{k})c_{\beta\nu}(\boldsymbol{k}), \quad (3)$$

where $c^\dagger_{\alpha\mu}(\boldsymbol{k})$ creates an itinerant electron with momentum $\boldsymbol{k}$, spin $\mu$ and orbital index $\alpha$. The Fermi surface of FeSe consists of two electron pockets around the M points and one hole pocket around the $\Gamma$ point.[28–30] Following,[6,48] we take a symmetry based approach and expand the dispersion around the Fermi surface. Experimentally $d_{yz}$ and $d_{zx}$ orbitals dominate the $\Gamma$ point, $d_{yz}$ and $d_{xy}$ dominate the $(\pi,0)$ point, and $d_{zx}$ and $d_{xy}$ dominate the $(0,\pi)$ point. So we consider the corresponding intra- and inter-orbital hopping terms. Furthermore we include on-site nematicity and spin-orbit coupling to produce the band splitting that gives rise to a single hole pocket around $\Gamma$. The resulting simplified Fermi surface is shown in Fig.4a, see SM2 for explicit parameters.[49]

We model the coupling between the itinerant electrons and the local moments via a Kondo-like coupling:[33]

$$\mathcal{H}_{\rm int} = -\sum_{i,\alpha,\mu\nu} J_\alpha \boldsymbol{S}_i\cdot c^\dagger_{i\alpha\mu}\boldsymbol{\sigma}_{\mu\nu}c_{i\alpha\nu}, \quad (4)$$

where $\boldsymbol{\sigma}$ represents the vector of Pauli matrices, and $J_\alpha > 0$ denote the Kondo-like couplings. The Kondo-like couplings are generally different for different orbitals. Hence we consider the implication of possible differences.[50]

The proposed nematic QSL state induces nematicity in the charge sector. For instance non-zero $\langle A_{\boldsymbol{r},\boldsymbol{r}\pm\hat x}\rangle$ in the nematic QSL state generates an interaction among conduction electrons along the $x$-direction, which drives bond-centered nematic order with $\varphi_c \equiv \langle c^\dagger_{\boldsymbol{r}+\hat x,\alpha}c_{\boldsymbol{r},\alpha} - c^\dagger_{\boldsymbol{r}+\hat y,\alpha}c_{\boldsymbol{r},\alpha}\rangle \neq 0$ below the temperature at which the nematic QSL develops. The observed nematic transition at $T_s \sim 90K$[8] is consistent with this picture. Furthermore, $\varphi_c$ linearly couples to $\varphi_o \equiv \frac{n_{zx}-n_{yz}}{n_{zx}+n_{yz}}$, where $n_{zx,yz}$ denote occupation of $zx$ and $yz$ orbitals, and $\varphi_s \equiv M_x^2 - M_y^2$, where $\boldsymbol{M}$ represents the magnetic moment. These different measures of nematicity are consistent with orbital imbalance observed in ARPES[28–30] ($\varphi_o \neq 0$) and the observed NMR resonance line splitting[51] ($\varphi_s \neq 0$).

The nematic spin fluctuations in the proposed QSL state mediate pairing. We determine the resulting gap structure via mean field procedure[53] . Remarkably, non-universal aspects of the gap structure such as relative gap strength of each pocket and the $T_c$ are sensitive to strength of the couplings $J$'s (see Fig. 4b,c). Nevertheless the gap functions share the following generic features: (1) The gap is nodeless since the anisotropy in the nematic QSL spin fluctuation removes any need for a node.

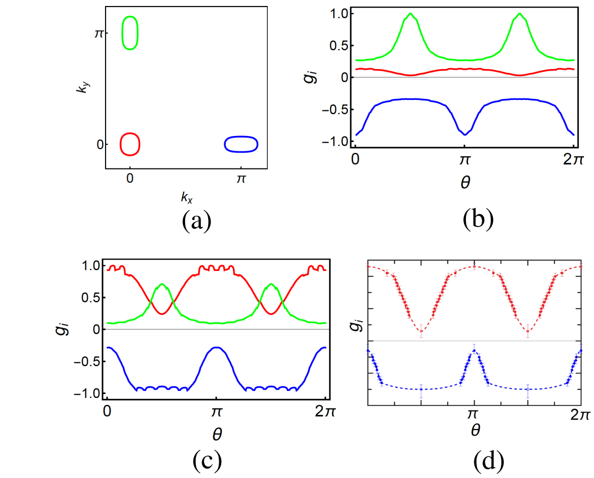


FIG. 4. (Color online) (a): The Fermi surface. (b, c): The gap symmetry function on different Fermi pockets for three-band models with $J_{yz} = J_{zx} = J_{xy} = 1$ (b) and $J_{yz} = J_{zx} = 1$, $J_{xy} = 0.4$ (c) and $J_1$-$J_2$-$J_3$-$J_4$ chosen in the vicinity of the shaded region of Fig. 3 (top). Note: we make no attempt to simultaneously fit STM data here and neutron data in Fig. 2 with the same model. (d): The gap function observed in the recent STM measurements.[52]

By contrast, in the itinerant model where $(\pi, \pi)$, $(\pi, 0)$ and $(0, \pi)$ spin fluctuations are close in magnitude they compete for deciding the sign structure of the gap causing nodal gap structures. (2) The gap deeply anisotropic due to the variation of orbital content around each Fermi pocket. The resulting nodeless but very anisotropic gap structure explains the seemingly contradictory experimental results of STM,[54,55] penetration depth,[55] thermal conductivity measurements,[56] observing low energy excitations[54,55] despite the evidence of a full gap.[52,56] (3) The gap changes sign from pocket to pocket. This is consistent (see SM4) with the observation of sharp spin resonance in the superconducting state.[57] More specifically, our gap function is a combination of $d$-wave as induced by $(\pi, \pi)$ spin fluctuations and $s_\pm$ as induced by $(\pi, 0)$ spin fluctuations (note that $S_z$-breaking spin-orbit coupling will mix the spin-singlet pairing considered here with an even parity spin-triplet pairing[48]). Two examples are shown in Fig.4b,c.

Fig. 4b,c shows that the orbital dependent Kondo-like coupling can alter the relative magnitude and anisotropy of gap functions at different Fermi pockets (while the gap is predominantly $d$-wave in Fig. 4b, $d$- and $s$-wave are at par in Fig. 4c). Since the Kondo-like coupling requires overlap of the wave-function between the conduction electrons and local moments, significantly lower spectral weight of $d_{xy}$ orbitals[58] implies $J_{xy} \ll J_{zx}, J_{yz}$.[59]

Indeed, the gap function with such orbital dependent Kondo-like coupling shows a compelling resemblance to the gap structure observed by recent STM measurements[52] (see Fig. 4c,d).Sprau et al.[52] incorporated the lower weights of $d_{xy}$ orbitals through the choice of $Z$-factors and showed that the calculated gap anistropy can be fit to experimental results using $Z$'s as fitting parameters while tuning interactions to Stoner instability. In our model, imbalance in the spectral weight is incorporated through the orbital dependence of the Kondo-like coupling $J_{xy} < J_{yz} = J_{zx}$. This orbital dependent Kondo-like coupling amplify the role of $(\pi, 0)$ spin fluctuation in pairing despite larger spectral weight at $(\pi, \pi)$, which is consistent with the observation of sharp spin resonance at $(\pi, 0)$[57] (see SM4 for further discussion).

In conclusion, we propose a nematic QSL state description of FeSe that explains the basic phenomenology of FeSe: (1) Spin dynamics observed in Ref.9 assuming it is averaged over domains, (2) nematic transition without mangetic ordering, (3) highly anisotropic fully gapped superconducting gap. The central assumption that neutron scattering is averaging over domains could be tested in a detwinned neutron experiment. Orbital dependent Kondo-like coupling mechanisms for orbital selective pairing in bulk FeSe further offers new insight regarding higher $T_c$ observed in mono-layer FeSe and K-doped FeSe. As we show in SM4, larger $J_{xy}$ that enables conduction electrons to utilize $(\pi, \pi)$ spin fluctuation with larger intensity and higher characteristic frequency leads to higher transition temperature (as high as 47K). Combined with the observation that spectral weight of the $d_{xy}$ orbitals in the conduction electrons is much higher in the higher $T_c$ settings of mono-layer FeSe and K-doped FeSe,[58] it is conceivable these systems make better use of already more prominent $(\pi, \pi)$ fluctuation to achieve higher $T_c$. We note here that the nematic QSL state we propose is distinct from the proposal of Ref. 17 in that it contains no one-magnon branch of excitations[60] although both proposals start from strong coupling perspective and spin ground states lacking any form of magnetic order. Finally, although we used SBMFT as a calculational crutch to capture the spinon continuum, the ultimate fate of spinons in this spin system coupled to itinerant electrons needs further study. Interestingly, such a state with spinons coexisting with conduction electrons would resemble the FL* state first proposed in Refs. 61 and 62 that has recently been revisited using DMRG.[63]

**Acknowledgements** We thank Andrey Chubukov, J.C. Davis, Rafael Fernandez, Peter Hirshfeld, Yong Baek Kim, Steve Kivelson, Dung-Hai Lee, Igor Mazin, Andriy Nevidomskyy, Subir Sachdev, Doug Scalapino, Qimiao Si, Fa Wang for discussions. E-AK and J-HS were supported by the U.S. Department of Energy, Office of Basic Energy Sciences, Division of Materials Science and Engineering under Award DE-SC0010313. E-AK also acknowledges Simons Fellow in Theoretical Physics Award#392182. E-AK and MJL acknowledge hospitality of the KITP supported by Grant No. NSF PHY11-25915.

[1] J. Paglione and R. L. Greene, Nature Physics **6**, 645 (2010), 1006.4618.

[2] P. J. Hirschfeld, M. M. Korshunov, and I. I. Mazin, Reports on Progress in Physics **74**, 124508 (2011), URL `http://stacks.iop.org/0034-4885/74/i=12/a=124508`.

[3] Q. Si, R. Yu, and E. Abrahams, Nature Reviews Materials **1**, 16017 (2016), 1604.03566.

[4] Q.-Y. Wang, Z. Li, W.-H. Zhang, Z.-C. Zhang, J.-S. Zhang, W. Li, H. Ding, Y.-B. Ou, P. Deng, K. Chang, et al., Chinese Physics Letters **29**, 037402 (2012), 1201.5694.

[5] F. Wang and D.-H. Lee, Science **332**, 200 (2011), ISSN 0036-8075, http://science.sciencemag.org/content/332/6026/200.full.pdf, URL `http://science.sciencemag.org/content/332/6026/200`.

[6] R. M. Fernandes and A. V. Chubukov, ArXiv e-prints (2016), 1607.00865.

[7] A. V. Chubukov, M. Khodas, and R. M. Fernandes, Phys. Rev. X **6**, 041045 (2016), URL `http://link.aps.org/doi/10.1103/PhysRevX.6.041045`.

[8] T. M. McQueen, A. J. Williams, P. W. Stephens, J. Tao, Y. Zhu, V. Ksenofontov, F. Casper, C. Felser, and R. J. Cava, Phys. Rev. Lett. **103**, 057002 (2009), URL `http://link.aps.org/doi/10.1103/PhysRevLett.103.057002`.

[9] Q. Wang, Y. Shen, B. Pan, X. Zhang, K. Ikeuchi, K. Iida, A. D. Christianson, H. C. Walker, D. T. Adroja, M. Abdel-Hafiez, et al., Nat Commun **7** (2016), URL `http://dx.doi.org/10.1038/ncomms12182`.

[10] S. Mukherjee, A. Kreisel, P. J. Hirschfeld, and B. M. Andersen, Phys. Rev. Lett. **115**, 026402 (2015), URL `http://link.aps.org/doi/10.1103/PhysRevLett.115.026402`.

[11] A. Kreisel, S. Mukherjee, P. J. Hirschfeld, and B. M. Andersen, Phys. Rev. B **92**, 224515 (2015), URL `http://link.aps.org/doi/10.1103/PhysRevB.92.224515`.

[12] R.-Q. Xing, L. Classen, M. Khodas, and A. V. Chubukov, ArXiv e-prints (2016), 1611.03912.

[13] L. Classen, R.-Q. Xing, M. Khodas, and A. V. Chubukov, ArXiv e-prints (2016), 1612.08708.

[14] H. Gretarsson, A. Lupascu, J. Kim, D. Casa, T. Gog, W. Wu, S. R. Julian, Z. J. Xu, J. S. Wen, G. D. Gu, et al., Phys. Rev. B **84**, 100509 (2011), URL `http://link.aps.org/doi/10.1103/PhysRevB.84.100509`.

[15] R. Yu and Q. Si, Phys. Rev. Lett. **115**, 116401 (2015), URL `http://link.aps.org/doi/10.1103/PhysRevLett.115.116401`.

[16] Z. Wang, W.-J. Hu, and A. H. Nevidomskyy, Phys. Rev. Lett. **116**, 247203 (2016), URL `http://link.aps.org/doi/10.1103/PhysRevLett.116.247203`.

[17] F. Wang, S. A. Kivelson, and D.-H. Lee, Nat Phys **11**, 959 (2015), URL `http://dx.doi.org/10.1038/nphys3456`.

[18] I. Affleck, T. Kennedy, E. H. Lieb, and H. Tasaki, Phys. Rev. Lett. **59**, 799 (1987), URL `https://link.aps.org/doi/10.1103/PhysRevLett.59.799`.

[19] J. K. Glasbrenner, I. I. Mazin, H. O. Jeschke, P. J. Hirschfeld, R. M. Fernandes, and R. Valenti, Nat Phys **11**, 953 (2015), URL `http://dx.doi.org/10.1038/nphys3434`.

[20] P. Chandra, P. Coleman, and A. I. Larkin, Phys. Rev. Lett. **64**, 88 (1990), URL `http://link.aps.org/doi/10.1103/PhysRevLett.64.88`.

[21] G. Misguich and C. Lhuillier, *Two-Dimensional Quantum Antiferromagnets* (World Scientific Publishing Co, 2004), pp. 229–306.

[22] R. M. Fernandes, L. H. VanBebber, S. Bhattacharya, P. Chandra, V. Keppens, D. Mandrus, M. A. McGuire, B. C. Sales, A. S. Sefat, and J. Schmalian, Phys. Rev. Lett. **105**, 157003 (2010), URL `https://link.aps.org/doi/10.1103/PhysRevLett.105.157003`.

[23] F. D. M. Haldane, Phys. Rev. Lett. **61**, 1029 (1988), URL `http://link.aps.org/doi/10.1103/PhysRevLett.61.1029`.

[24] N. Read and S. Sachdev, Phys. Rev. B **42**, 4568 (1990), URL `http://link.aps.org/doi/10.1103/PhysRevB.42.4568`.

[25] H. C. Jiang, F. Krüger, J. E. Moore, D. N. Sheng, J. Zaanen, and Z. Y. Weng, Phys. Rev. B **79**, 174409 (2009), URL `http://link.aps.org/doi/10.1103/PhysRevB.79.174409`.

[26] H.-C. Jiang, H. Yao, and L. Balents, Phys. Rev. B **86**, 024424 (2012), URL `http://link.aps.org/doi/10.1103/PhysRevB.86.024424`.

[27] S.-S. Gong, W. Zhu, D. N. Sheng, and K. Yang, ArXiv e-prints (2016), 1606.00937.

[28] K. Nakayama, Y. Miyata, G. N. Phan, T. Sato, Y. Tanabe, T. Urata, K. Tanigaki, and T. Takahashi, Phys. Rev. Lett. **113**, 237001 (2014), URL `http://link.aps.org/doi/10.1103/PhysRevLett.113.237001`.

[29] M. D. Watson, T. K. Kim, A. A. Haghighirad, N. R. Davies, A. McCollam, A. Narayanan, S. F. Blake, Y. L. Chen, S. Ghannadzadeh, A. J. Schofield, et al., Phys. Rev. B **91**, 155106 (2015), URL `http://link.aps.org/doi/10.1103/PhysRevB.91.155106`.

[30] Y. Suzuki, T. Shimojima, T. Sonobe, A. Nakamura, M. Sakano, H. Tsuji, J. Omachi, K. Yoshioka, M. Kuwata-Gonokami, T. Watashige, et al., Phys. Rev. B **92**, 205117 (2015), URL `http://link.aps.org/doi/10.1103/PhysRevB.92.205117`.

[31] S. J. Moon, J. H. Shin, D. Parker, W. S. Choi, I. I. Mazin, Y. S. Lee, J. Y. Kim, N. H. Sung, B. K. Cho, S. H. Khim, et al., Phys. Rev. B **81**, 205114 (2010), URL `http://link.aps.org/doi/10.1103/PhysRevB.81.205114`.

[32] S.-P. Kou, T. Li, and Z.-Y. Weng, EPL (Europhysics Letters) **88**, 17010 (2009), URL `http://stacks.iop.org/0295-5075/88/i=1/a=17010`.

[33] W. Lv, F. Krüger, and P. Phillips, Phys. Rev. B **82**, 045125 (2010), URL `http://link.aps.org/doi/10.1103/PhysRevB.82.045125`.

[34] W.-G. Yin, C.-C. Lee, and W. Ku, Phys. Rev. Lett. **105**, 107004 (2010), URL `http://link.aps.org/doi/10.1103/PhysRevLett.105.107004`.

[35] V. Stanev and P. B. Littlewood, Phys. Rev. B **87**, 161122 (2013), URL `http://link.aps.org/doi/10.1103/PhysRevB.87.161122`.

[36] S. Liang, A. Mukherjee, N. D. Patel, C. B. Bishop, E. Dagotto, and A. Moreo, Phys. Rev. B **90**, 184507 (2014), URL `http://link.aps.org/doi/10.1103/PhysRevB.90.184507`.

[37] D.-H. Lee, Chinese Physics B **24**, 117405 (2015), URL `http://stacks.iop.org/1674-1056/24/i=11/a=117405`.

[38] C. Fang, H. Yao, W.-F. Tsai, J. Hu, and S. A. Kivelson, Phys. Rev. B **77**, 224509 (2008), URL `http://link.aps.org/doi/10.1103/PhysRevB.77.224509`.

[39] C. Xu, M. Müller, and S. Sachdev, Phys. Rev. B **78**, 020501 (2008), URL `http://link.aps.org/doi/10.1103/PhysRevB.78.020501`.

[40] L. Balents, Nature **464**, 199 (2010).

[41] D. P. Arovas and A. Auerbach, Phys. Rev. B **38**, 316 (1988), URL `http://link.aps.org/doi/10.1103/PhysRevB.38.316`.

[42] G. Müller, H. Thomas, H. Beck, and J. C. Bonner, Phys. Rev. B **24**, 1429 (1981), URL `http://link.aps.org/doi/10.1103/PhysRevB.24.1429`.

[43] B. Lake, D. A. Tennant, J.-S. Caux, T. Barthel, U. Schollwöck, S. E. Nagler, and C. D. Frost, Phys. Rev. Lett. **111**, 137205 (2013), URL `http://link.aps.org/doi/10.1103/PhysRevLett.111.137205`.

[44] R. Vlijm and J.-S. Caux, Journal of Statistical Mechanics: Theory and Experiment **5**, 05009 (2014), 1401.4450.

[45] S. Sachdev and N. Read, International Journal of Modern Physics B **5**, 219 (1991), cond-mat/0402109.

[46] O. Tchernyshyov, R. Moessner, and S. L. Sondhi, EPL (Europhysics Letters) **73**, 278 (2006), cond-mat/0408498.

[47] A. Auerbach and D. P. Arovas, Phys. Rev. Lett. **61**, 617 (1988), URL `http://link.aps.org/doi/10.1103/PhysRevLett.61.617`.

[48] V. Cvetkovic and O. Vafek, Phys. Rev. B **88**, 134510 (2013), URL `http://link.aps.org/doi/10.1103/PhysRevB.88.134510`.

[49] Our rather simple band structure allows largely analytic calculation at the expense of missing out quantiative details such as large mismatch in the pocket sizes as found in quantum oscillation (see SM4).

[50] As discussed in SM3, coupling to itinerant electrons generates a self-energy for the local moment propagator, giving rise to Landau damping. However the strength of the Kondo-like couplings can be estimated to be much weaker than the spin exchange interaction. Hence coupling to itinerant electrons will not significantly modify the local moment spin susceptibility. SM3 includes Ref..[64]

[51] S.-H. Baek, D. V. Efremov, J. M. Ok, J. S. Kim, J. van den Brink, and B. Büchner, Nat Mater **14**, 210 (2015), URL `http://dx.doi.org/10.1038/nmat4138`.

[52] P. O. Sprau, A. Kostin, A. Kreisel, A. E. Böhmer, V. Taufour, P. C. Canfield, S. Mukherjee, P. J. Hirschfeld, B. M. Andersen, and J. C. Séamus Davis, ArXiv e-prints (2016), 1611.02134.

[53] See Supplemental Material SM4 for a detail discussion of the mean field theory, which includes Refs..[65–71]

[54] C.-L. Song, Y.-L. Wang, P. Cheng, Y.-P. Jiang, W. Li, T. Zhang, Z. Li, K. He, L. Wang, J.-F. Jia, et al., Science **332**, 1410 (2011), ISSN 0036-8075, http://science.sciencemag.org/content/332/6036/1410.full.pdf, URL `http://science.sciencemag.org/content/332/6036/1410`.

[55] S. Kasahara, T. Watashige, T. Hanaguri, Y. Kohsaka, T. Yamashita, Y. Shimoyama, Y. Mizukami, R. Endo, H. Ikeda, K. Aoyama, et al., Proceedings of the National Academy of Sciences **111**, 16309 (2014), http://www.pnas.org/content/111/46/16309.full.pdf, URL `http://www.pnas.org/content/111/46/16309.abstract`.

[56] P. Bourgeois-Hope, S. Chi, D. A. Bonn, R. Liang, W. N. Hardy, T. Wolf, C. Meingast, N. Doiron-Leyraud, and L. Taillefer, Phys. Rev. Lett. **117**, 097003 (2016), URL `http://link.aps.org/doi/10.1103/PhysRevLett.117.097003`.

[57] Q. Wang, Y. Shen, B. Pan, Y. Hao, M. Ma, F. Zhou, P. Steffens, K. Schmalzl, T. R. Forrest, M. Abdel-Hafiez, et al., Nature Materials **15**, 159 (2016), 1502.07544.

[58] M. Yi, Z.-K. Liu, Y. Zhang, R. Yu, J.-X. Zhu, J. J. Lee, R. G. Moore, F. T. Schmitt, W. Li, S. C. Riggs, et al., Nature Communications **6**, 7777 (2015), 1506.03888.

[59] Since the relative magnitudes of $J$'s are not symmetry-constrained, it is reasonable to expect $J_{xy}$ to be different from $J_{zx}$ and $J_{yz}$. A desirable principles-based study of the $J$'s is underway.

[60] See Supplemental Material SM4 for a detail comparison between the nematic QSL and that of Ref.,[17] which includes Refs..[72–76]

[61] T. Senthil, S. Sachdev, and M. Vojta, Phys. Rev. Lett. **90**, 216403 (2003), URL `http://link.aps.org/doi/10.1103/PhysRevLett.90.216403`.

[62] T. Senthil, M. Vojta, and S. Sachdev, Phys. Rev. B **69**, 035111 (2004), URL `http://link.aps.org/doi/10.1103/PhysRevB.69.035111`.

[63] J. Lee, S. Sachdev, and S. R. White, Phys. Rev. B **94**, 115112 (2016), URL `http://link.aps.org/doi/10.1103/PhysRevB.94.115112`.

[64] D. J. Scalapino, Rev. Mod. Phys. **84**, 1383 (2012), URL `https://link.aps.org/doi/10.1103/RevModPhys.84.1383`.

[65] D. A. Kirzhnits, E. G. Maksimov, and D. I. Khomskii, Journal of Low Temperature Physics **10**, 79 (1973), ISSN 1573-7357, URL `http://dx.doi.org/10.1007/BF00655243`.

[66] S. N. Klimin, J. Tempere, J. T. Devreese, and D. van der Marel, Phys. Rev. B **89**, 184514 (2014), URL `http://link.aps.org/doi/10.1103/PhysRevB.89.184514`.

[67] S. Kasahara, T. Watashige, T. Hanaguri, Y. Kohsaka, T. Yamashita, Y. Shimoyama, Y. Mizukami, R. Endo, H. Ikeda, K. Aoyama, et al., Proceedings of the National Academy of Sciences **111**, 16309 (2014), http://www.pnas.org/content/111/46/16309.full.pdf, URL `http://www.pnas.org/content/111/46/16309.abstract`.

[68] Y. Miyata, K. Nakayama, K. Sugawara, T. Sato, and T. Takahashi, Nat Mater **14**, 775 (2015), URL `http://dx.doi.org/10.1038/nmat4302`.

[69] J. J. Lee, F. T. Schmitt, R. G. Moore, S. Johnston, Y. T. Cui, W. Li, M. Yi, Z. K. Liu, M. Hashimoto, Y. Zhang, et al., Nature **515**, 245 (2014), URL `http://dx.doi.org/10.1038/nature13894`.

[70] N. Bulut, D. J. Scalapino, and R. T. Scalettar, Phys. Rev. B **45**, 5577 (1992), URL `https://link.aps.org/doi/10.1103/PhysRevB.45.5577`.

[71] T. Terashima, N. Kikugawa, A. Kiswandhi, E.-S. Choi, J. S. Brooks, S. Kasahara, T. Watashige, H. Ikeda, T. Shibauchi, Y. Matsuda, et al., Phys. Rev. B **90**, 144517 (2014), URL `https://link.aps.org/doi/10.1103/PhysRevB.90.144517`.

[72] A. Läuchli, G. Schmid, and S. Trebst, Phys. Rev. B **74**, 144426 (2006), URL `http://link.aps.org/doi/10.1103/PhysRevB.74.144426`.

[73] S. R. Manmana, A. M. Läuchli, F. H. L. Essler, and F. Mila, Phys. Rev. B **83**, 184433 (2011), URL `http://link.aps.org/doi/10.1103/PhysRevB.83.184433`.

[74] A. Schmitt, K.-H. Mütter, M. Karbach, Y. Yu, and G. Müller, Phys. Rev. B **58**, 5498 (1998), URL `http://link.aps.org/doi/10.1103/PhysRevB.58.5498`.

[75] L. A. Takhtajan, Phys. Lett. **A87**, 479 (1982).

[76] H. M. Babujian, Phys. Lett. **A90**, 479 (1982).